CAMS Service Evolution

D1.2 Report on operational AVRAS experiment

Due date of deliverable	30 November 2025
Submission date	9th December 2025
File Name	CAMEO_D1.2_v1.0
Work Package /Task	WP1 Task 1.1
Organisation Responsible of Deliverable	ECMWF
Author name(s)	Samuel Quesada-Ruiz, Angela Benedetti, Cristina Lupu, Tobias Necker
Revision number	1.0
Status	Issued
Dissemination Level	PUBLIC

Funded by the European Union

The CAMEO project (grant agreement No 101082125) is funded by the European Union.
Views and opinions expressed are however those of the author(s) only and do not necessarily reflect those of the European Union or the Commission. Neither the European Union nor the granting authority can be held responsible for them.

1 Executive Summary

This report describes the months 19-35 of activity related to the implementation of a prototype assimilation system for aerosol-affected visible radiances (AVRAS) within the Integrated Forecasting System's 4D-Var in atmospheric composition configuration (IFS-COMPO). The objective of this report is to document the progress made in the completion of the WP1 objectives and to highlight initial results from monitoring and assimilation experiments, as planned in Task 1.1.

The efforts have primarily concentrated on developing the new infrastructure, in a configuration that closely mirror the IFS-COMPO operational setup, with focus on five main aspects:

(i) the implementation and testing of the neural network (NN) based version MFASIS-Aerosol fast radiative transfer code to compute aerosol reflectances;
(ii) the selection of observations to be used;
(iii) the preparation of the visible reflectance observations and their encoding into a Binary Universal Form for the Representation of meteorological data (BUFR) template created for this purpose;
(iv) the configuration setup and running of the assimilation experiments;
(v) the evaluation of the assimilation results.

The fast radiative transfer code for aerosol reflectances MFASIS-Aerosol (Method for Fast Satellite Image Synthesis) was successfully integrated in cycle CY49R1 configuration, also upgraded to use the latest release of RTTOV version 14.0. This includes the forward operator together with the tangent linear and adjoint operators. The adjoint test, a mandatory requirement for the 4D-Var data assimilation, was verified and satisfied up to machine precision.

The option to use level 1 visible reflectances and screen the cloud-affected pixels using a thresholding method was ultimately set aside, and preference was instead given to using level 2 cloud-cleared visible reflectances provided by NASA for the MODIS instruments on Aqua and Terra. Cloud-cleared level 2 reflectances for the 665nm channel were extracted and converted to a BUFR sequence file specific to visible reflectances. This process was embedded in a script that can be run online within the IFS, allowing to run experiments for any period where the data is available without any additional pre-processing. It is worth noting that this approach can be applied to any instruments and it is not unique to MODIS, provided the reflectances are cloud-cleared.

Assimilation experiments were run for two distinct periods, May and June 2025. For each period, the experimentation included the assimilation of visible reflectances using two different estimates for observation error variances, along with a control experiment (i.e., no Aerosol Optical Depth (AOD) assimilated) and a baseline experiment (i.e. assimilation of AOD as in CAMS operations).

The evaluation results and main achievements are shown in this report. First, the implementation of substantial technical developments enabling visible reflectance monitoring and assimilation within the Integrated Forecasting System (IFS) was achieved according to the Task 1.1 objectives. These include the integration of MFASIS-Aerosols, the adaptation of RTTOV-14.0 interfaces, and the creation of a bespoke data flows for aerosol-related visible observations. Second, this is the first successful demonstration of aerosol visible monitoring and assimilation using the RTTOV-MFASIS framework, showcasing an improved aerosol

representation and reduced observation-model discrepancies in case studies such as the Saharan dust outbreak of 4th June 2025.

There are some caveats in the elements used in this experimentation, which render the configuration of these experiments suboptimal. Therefore, the findings presented here should be interpreted as a proof of concept for assimilating aerosol-affected visible reflectances, rather than as definitive scientific conclusions.

Table of Contents

2 Introduction

2.1 Background

Monitoring the composition of the atmosphere is a key objective of the European Union's flagship Space programme Copernicus, with the Copernicus Atmosphere Monitoring Service (CAMS) providing free and continuous data and information on atmospheric composition.

The CAMS Service Evolution (CAMEO) project has been funded to enhance the quality and efficiency of the CAMS service and help CAMS to better respond to policy needs such as air pollution and greenhouse gases monitoring, the fulfilment of sustainable development goals, and sustainable and clean energy.

In the context of aerosol reflectance assimilation, progress towards assimilating visible radiances had been made within the Aerosol Radiance Assimilation Study (ARAS) project funded by the European Space Agency (ESA) from 2018 to 2020. It was shown that the assimilation of aerosol visible radiances increased the aerosol load in the analysis to a level comparable to the MODIS aerosol optical depth data (see Figure 1) and improved other aerosol parameters as well (not shown). The visible reflectance operator used in ARAS did not reach operational maturity.

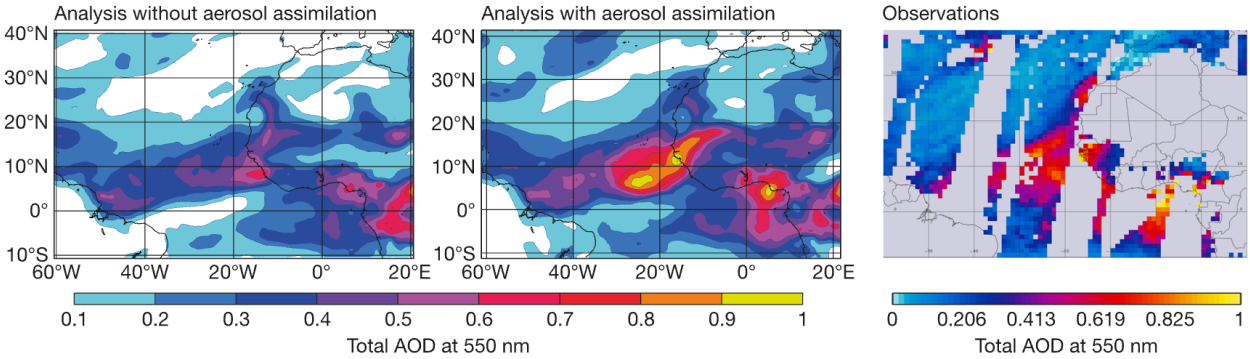

Figure 1. Total AOD at 550 nm analysis without any assimilated aerosol data (left) and with the assimilation of MODIS aerosol visible reflectances at two different wavelengths (665 nm and 866 nm, middle), compared to total AOD from MODIS at 550 nm (right). More information on this study can be found in Benedetti et al 2020 (https://www.ecmwf.int/en/newsletter/162/news/progress-towards-assimilating-visible-radiances)

Simulation of the Flexible Combine Imager (FCI) images using high-resolution forecasts (9 km fields from the IFS operational model run) fed to our radiative transfer facility capable of producing visible images show a good performance when compared to observations, but there is a clear lack of aerosol information. As an example, we can see in Figure 2 that the Saharan dust travelling over the Atlantic is missing in the simulated reflectances. This aspect has been addressed in Task 1.1.

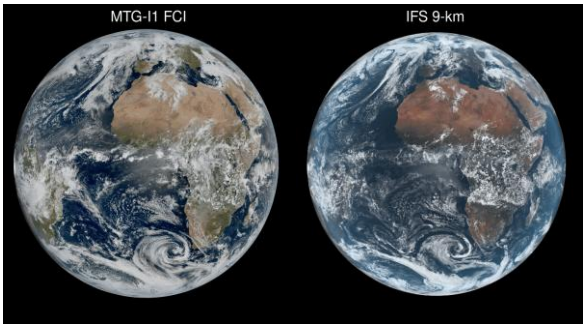

Figure 2. *MTG-I1 FCI observations (left) vs IFS-9km reflectances simulated using RTTOV MFASIS-Cloud (right). Credits: Philippe Lopez (ECMWF).*

2.2 Scope of this deliverable

2.2.1 Objectives of this deliverable

This report describes the months 19-35 of activity related to the implementation of a prototype assimilation system for aerosol-affected visible radiances within the ECMWF IFS-COMPO. The work involved a series of systematic modifications to ensure the developments fully support the requirements of aerosols visible radiance assimilation. The objective of this report is to record the progress made so far and to highlight initial results from the monitoring and assimilation experiments as planned in Task 1.1.

2.2.2 Work performed in this deliverable

In this deliverable, the work as planned in the Description of Action (DoA, WP1 T1.1) was performed. Key activities included:

1. implementing and testing of the MFASIS-Aerosol fast radiative transfer code for aerosol visible reflectances
2. handling cloud contamination in visible-channel aerosol assimilation
3. implementing an observation processing data flow for cloud-cleared aerosol-affected visible reflectance observations
4. setting up and running assimilation experiments
5. evaluating the assimilation results.

The next sections will discuss these five points in detail.

2.2.3 Deviations and countermeasures

No deviations have been made.

3 Integration of MFASIS-Aerosol in the IFS

Assimilation of visible aerosol reflectances in numerical weather prediction (NWP) and atmospheric composition models requires a radiative transfer operator capable of accurately and efficiently simulating top-of-atmosphere reflectances. Traditional radiative transfer solvers for aerosols are line-by-line models (e.g., Discrete Ordinate Method -DOM), that while very accurate, are computationally overly expensive and impractical for large-scale data assimilation systems that require repeated simulations with the forward, tangent linear, and adjoint operators.

MFASIS is a fast and accurate approximation of the 1D radiative transfer model DOM for the simulation of reflectances for satellite channels in the solar range. It has reduced computational costs, making these spectral regions relevant to NWP systems. Since its first implementation in the radiative transfer code used operationally at several NWP centres (RTTOV, https://nwp-saf.eumetsat.int/site/software/rttov/documentation), MFASIS is continuously being developed to further increase accuracy and to extend capabilities. Examples of this are the introduction of neural-network-based (MFASIS-NN) (Scheck, 2021) solver for cloudy visible reflectances, and the application of MFASIS-NN to scattering by aerosols. RTTOV simulations require sensor-specific files containing information related to the sensor, including coefficients for the gas optical depth parameterisation, scattering optical properties, and coefficients for the MFASIS-NN fast neural-network-based parameterisation for visible/near-IR scattering simulations.

The implementation and evaluation of RTTOV-14.0 (which will become operational in IFS at cycle 50r1) have been successfully completed. The transition in the IFS from RTTOV-13.2 to RTTOV-14.0 involved significant changes in the interface and introduced new science capabilities that pave the way for future developments. Relevant for this project, it allowed the pre-beta testing of elements of RTTOV-14.1, which have not yet been released (e.g., MFASIS-Aerosol, available only to ECMWF since September 2024). Scattering simulations require additional input files containing the scattering optical properties for aerosols. In March 2025, an example of MFASIS-NN dedicated coefficient file for handling simulations involving aerosols (e.g., SEVIRI/Meteosat-11) was provided to ECMWF for testing.

MFASIS-Aerosol was designed for the direct assimilation of aerosol reflectances in the visible and near-infrared, where aerosol scattering dominates. The scientific motivation for integrating RTTOV MFASIS-Aerosols in the IFS-COMPO includes:

- **Enhanced aerosol characterization**: visible reflectances are highly sensitive to aerosol optical depth, size distribution, and composition, offering complementary information to AOD retrievals.
- **Improved air quality forecasts**: better aerosol initial conditions lead to better CAMS forecasts.
- **Improved NWP forecast skill**: better aerosol initial conditions can influence shortwave radiation, surface energy balance, and ultimately weather forecasts.
- **Operational feasibility**: the fast approximation ensures that assimilation of reflectances can be performed within the time constraints of operational NWP/CAMS cycles.
- **Consistency with variational assimilation**: MFASIS-Aerosols provides not only the forward operator but also tangent linear and adjoint capabilities, which are essential for 4D-Var and hybrid assimilation frameworks. Assumptions done in the satellite aerosol retrievals can be inconsistent with IFS-COMPO, while in this exercise, the alignment of the assumption, despite not perfect, is more consistent.
- **Possibility of assimilating multiple shortwave sensors simultaneously**, extracting their full information content. This represents an advantage compared to retrievals based on each sensor independently, as the quality of these rely heavily on elements such as viewing geometry, orbits or missing channels. Additionally, the direct use of calibrated reflectances does not suffer from inter-product biases as it could happen with products which have been developed independently with their own set of assumptions.

By enabling the assimilation of aerosol-affected visible reflectances, MFASIS-Aerosol represents a significant step toward exploiting the full information content of satellite observations for aerosol modelling and assimilation, thereby improving the representation of aerosol optical properties and spatial distribution in the analysis, as well as the coupling between atmospheric composition and meteorology.

The current version of MFASIS-Aerosol takes as input a vertical profile of atmospheric pressures, temperatures, humidities and aerosols along with information about the surface, and it outputs top of atmosphere satellite-seen reflectances (see schematic representation in Figure 3). MFASIS-Aerosol follows a similar approach as the cloud version (MFASIS-Cloud), where neural networks are trained with reflectances computed with the discrete ordinate method for simplified profiles that are defined by few parameters. The aerosol content from the original CAMS-based profile is represented in the simplified profile by concentrating the 9

CAMS-species defined in RTTOV (i.e., three bins for sea salt depending on size (0.03–0.5, 0.5–5 and 5–20 µm, SSA), three bins for dust (0.030–0.55, 0.55–0.9 and 0.9–20 µm, DUS), sulphate (SULP), hydrophilic organic matter (OMAT), and hydrophobic black carbon (BCAR)) into two distinct layers. This approach captures boundary-layer aerosols and a middle-to-upper tropospheric plume while preserving the total vertical integral of the aerosol loading.

Recent developments in RTTOV include a database of profiles for the 16 aerosol species used by CAMS in CY49R1 (Turner, 2025). Future re-training of MFASIS-Aerosols will make use of the 16 species description to improve the modelling of the aerosol reflectances.

The integration of the newly developed MFASIS-Aerosol operator, along with TL/AD versions at cycle CY49R1, led to a first successful analysis of aerosol-affected cloud-screened visible radiances from the MODIS sensors within IFS-COMPO. The adjoint test was performed and verified, confirming the correctness of the implementation and its suitability for assimilation experiments.

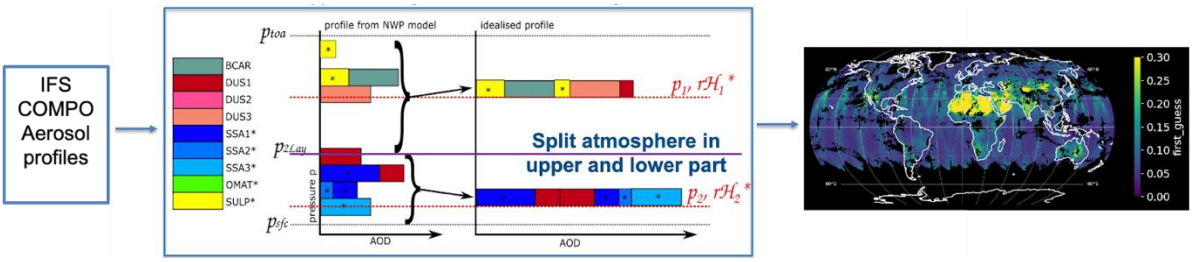

Figure 3. *Schematic example of an aerosol profile from a NWP model and the corresponding idealized profile representation in MFASIS-Aerosol in which only two layers are filled with aerosols.*

4 Handling cloud contamination in visible-channel aerosol assimilation

Assimilation of visible aerosol reflectances requires careful treatment of cloud contamination, as clouds strongly influence observed reflectances and can lead to significant biases if not properly accounted for. Three potential approaches for handling cloud contamination in visible reflectance assimilation have been identified:

1. **Apply in-house cloud screening:** This approach relies on applying a cloud detection algorithm prior to assimilation to exclude observations affected by clouds. However, Level-1 reflectance observations typically lack explicit information to discriminate clouds from aerosols. Using only model-based cloud information for screening introduces the risk of aliasing observed clouds into model aerosols, potentially degrading the analysis. While conceptually straightforward, this method depends heavily on the accuracy of the cloud mask and may not fully eliminate cloud contamination.
2. **Simultaneous assimilation of clouds and aerosols:** A more advanced strategy involves the joint assimilation of cloud and aerosol properties by constructing a combined observation operator. The concept is to simulate reflectances from two separate runs - one using MFASIS-Cloud and another using MFASIS-Aerosol - and combine them by subtracting the clear-sky surface reflectance once. This could potentially be a proxy for allowing the assimilation system to account for both aerosol and cloud contributions to observed reflectances. However, this approach is currently not feasible without major developments in RTTOV, as the system does not support loading two MFASIS neural network coefficient files simultaneously (ie. those for clouds required by MFASIS-Cloud and those for aerosols required by MFASIS-

Aerosol). Implementing this capability would require significant changes to RTTOV's architecture. Should an MFASIS-Cloud+Aerosol operator be developed, this approach could be reconsidered.

3. **Use cloud-cleared observations:** The most practical option is to use Level-2 cloud-cleared aerosol reflectances. Currently, such Level-2 products are available based on observations from MODIS instrument on Aqua and Terra or from the VIIRS instrument on the NOAA polar-orbiting satellites. This approach leverages existing cloud-clearing algorithms and minimizes the risk of cloud aliasing, making it attractive for a possible operational implementation. This approach was retained and applied within this project, using Level-2 cloud-cleared MODIS observations from the Collection 6.1.

5 Observation processing data flow

A custom data processing workflow was established to pre-process visible aerosol reflectance data from MODIS, facilitating their integration within the IFS and enabling their monitoring and assimilation.

The level-2 cloud-cleared aerosol reflectance product provided by the MODIS instruments on Aqua and Terra is encoded at ECMWF using a dedicated BUFR template for the AOD-related stream (e.g., reo3_aod). MODIS reflectances at 665nm are extracted from this BUFR AOD-sequence and converted into a local BUFR template, dedicated to the visible reflectances processing. These extraction and conversion steps were embedded in a script that can run online within the IFS environment. This enables experiments to be conducted for any MODIS-accessible period, without requiring additional pre-processing.

Superobbing techniques are applied to reduce data volume, to ensure consistency with the model at the analysis scale (TL511 ~40km), and to minimise the impacts of possible horizontal correlations on the observation error. This process computes the average of all MODIS reflectances within a model grid box, ensuring computational efficiency while preserving representativeness. In the current version of the IFS-COMPO CY49R1, MODIS reflectances were experimentally superobbed at a resolution of 80 km.

Processed observations are converted to ODB format for ingestion to the IFS (via the task bufr2odb). ODB is the in-house data storage system that enables the 4D-Var assimilation framework within IFS to store and access observational data efficiently.

6 Description of assimilation experiments

Assimilation experiments were conducted for two distinct periods: May 2025 and June 2025, to evaluate the impact of assimilating visible aerosol reflectances under varying observation error assumptions and to compare these results against the control configuration. All experiments were performed using IFS-COMPO cycle CY49R1, which was run at a horizontal spectral resolution of TL511 (equivalent to a grid size of about 40 km) and comprises 137 atmospheric levels (0.01 to 1013 hPa). An incremental 4D-Var assimilation scheme is applied to both meteorological and atmospheric composition variables using a 12 h assimilation window. In the IFS-COMPO configuration, the 12 h assimilation windows are defined from 03:00 to 15:00 UTC (denoted 12Z) and from 15:00 to 03:00 UTC (denoted 00Z).

The experimental framework comprised four configurations for each period (see Table 1):

1. **Control** – No assimilation of AOD or visible aerosol reflectances.

2. **Sensitivity Tests** – Assimilation of visible aerosol reflectances from MODIS Terra/Aqua over sea only (VIS_AER_RFL) using two fixed values of standard deviation of observation error:
    - **0.05**, representing a higher assumed uncertainty (ie, giving less weight to the observations). This was the value used in a previous study -ARAS, see Sect 2.1.
    - **0.015**, representing a lower assumed uncertainty (ie, giving more weight to the observations). This value was estimated using departure statistics (Desroziers et al 2005).
3. **Baseline** – Assimilation of AOD as in CAMS operations -this includes AOD observations from MODIS, PMAp and VIIRS.

This design allows assessment of the benefit of assimilating visible reflectances compared to control assimilation and a test of the sensitivity of the assimilation system to observation error specification.

Table 1. Summary of experiment configurations: each row provides the unique experiment ID, execution period, indicates whether AOD or VIS_AER_RFL was assimilated, and includes a description of the experimental setup.

expid	period	AOD	VIS_AER_RFL	Description
ivh0	May 2025	No	No	Control
iyip	May 2025	No	Yes	VIS_AER_RFL_0.05 (obs_error 0.05)
iyio	May 2025	No	Yes	VIS_AER_RFL_0.015 (obs_error 0.015)
ivpw	May 2025	Yes	No	Baseline
ivgy	June 2025	No	No	Control
iyin	June 2025	No	Yes	VIS_AER_RFL_0.05 (obs_error 0.05)
iyim	June 2025	No	Yes	VIS_AER_RFL_0.015 (obs_error 0.015)
ivpx	June 2025	Yes	No	Baseline

7 Evaluation results

7.1 Data selection

Cloud contamination is a big problem for aerosol assimilation, as cloud signals are an order of magnitude larger than the aerosol signal. Therefore, it is of paramount importance to screen clouds properly to avoid aliasing cloud signals into the aerosol analysis. Cloud screening has been addressed by using cloud-cleared level-2 reflectances.

Observation quality control is a critical step in the assimilation of visible reflectances, as unfiltered data can introduce significant biases due to surface and geometric effects. For the 665 nm channel, several selection criteria were applied to ensure data quality and representativeness:

- **Ocean-only observations**: Restricting data to ocean surfaces minimizes variability in surface reflectance and reduces uncertainties associated with land surface properties.
- **Sunglint exclusion**: Observations affected by sunglint were removed to avoid contamination from specular reflection, which can dominate the signal in certain viewing geometries. Sunglint filtering is applied over the sea only and is purely geometrical, based on a cut-off angle of 20 degrees.
- **Sea ice masking**: Reflectances over sea ice, based on the model information, were excluded due to their high albedo and strong contrast with open water, which can lead to misinterpretation in aerosol assimilation (and retrievals).
- **Solar and satellite zenith angle thresholds**: Observations with large solar zenith above 70 degrees or satellite zenith angles above 50 degrees were discarded to reduce errors associated with extreme viewing geometries and increased path length.

These criteria collectively enhance the reliability of assimilated reflectances by reducing systematic biases and improving consistency with model assumptions. The data selection and the impact of the quality control are illustrated in

a ALL MODIS AQUA/TERRA Observations

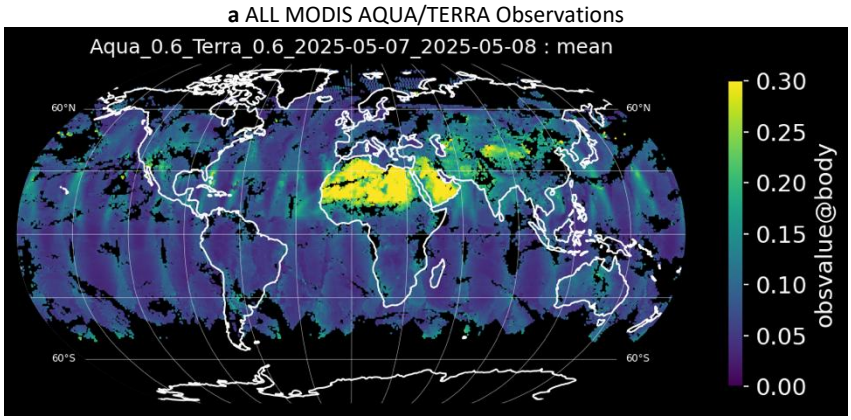

b ACTIVE MODIS AQUA/TERRA Observations

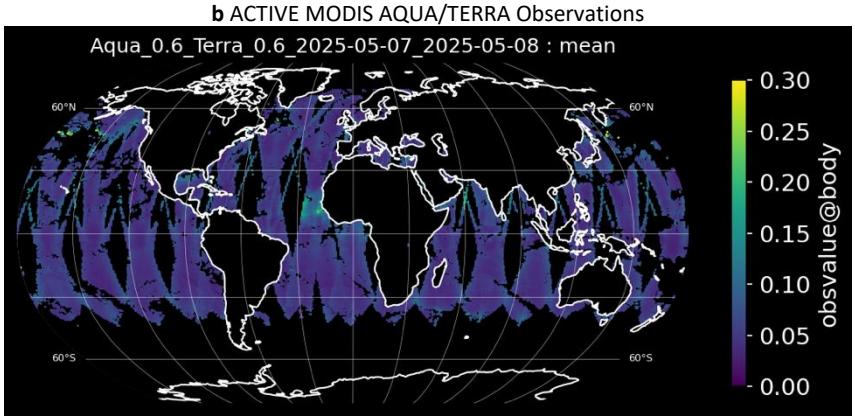

Figure **4** for the 8th May 2025.

Overall, from the ~5.5 million observations available after superobbing for each month, 33% were kept for May and 36% for June.

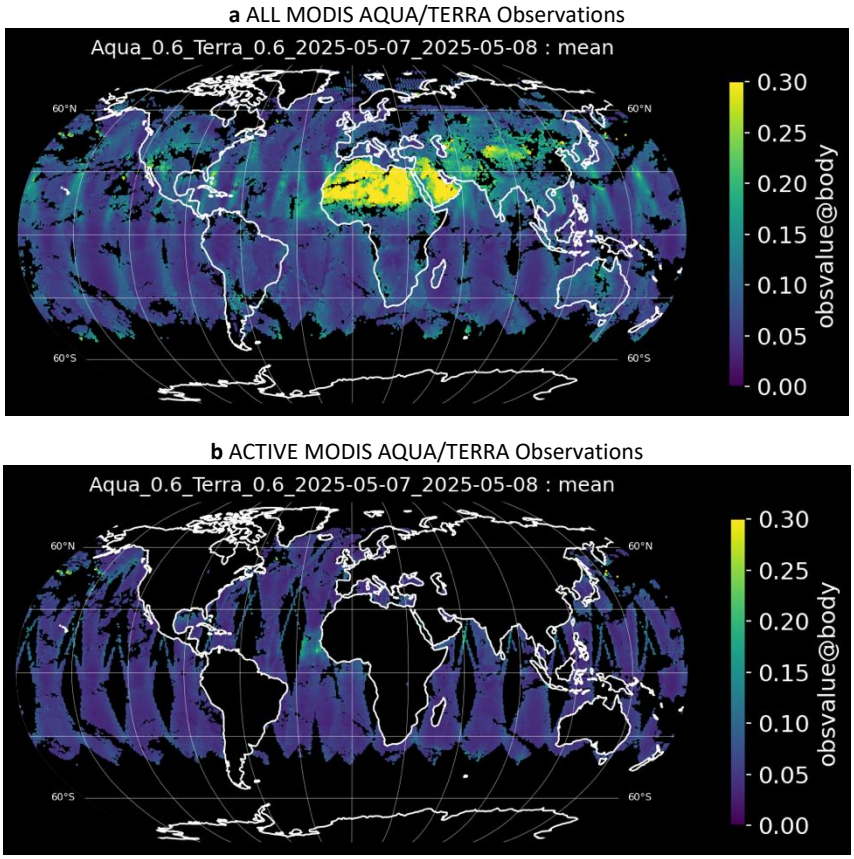

Figure 4. *Data selection applied to MODIS on Aqua and Terra observations on 8th May 2025.*

7.2 Monitoring

The data selection criteria described in Section 7.1 were applied to all assimilation experiments to ensure high-quality observations. The effect of this screening on the first guess departures, defined as the difference between the observation and its model equivalent, is illustrated in

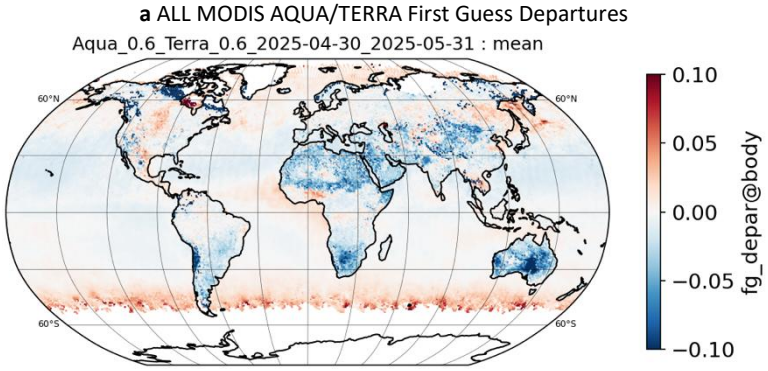

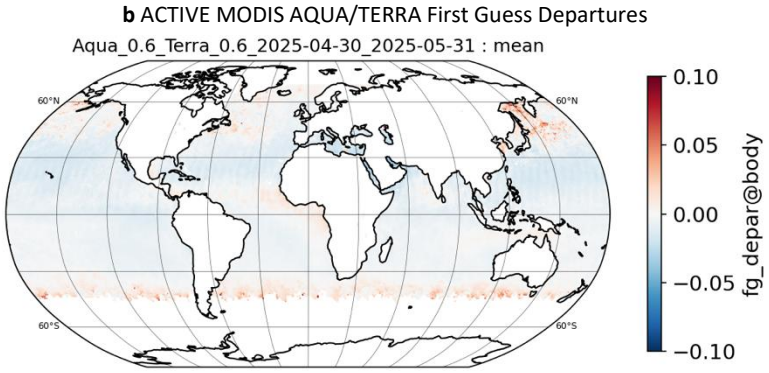

Figure **5**. This comparison highlights the importance of rigorous observation filtering for visible reflectances at 665 nm, as screening significantly reduces outliers and systematic biases, thereby improving the consistency of assimilated data with the model background.

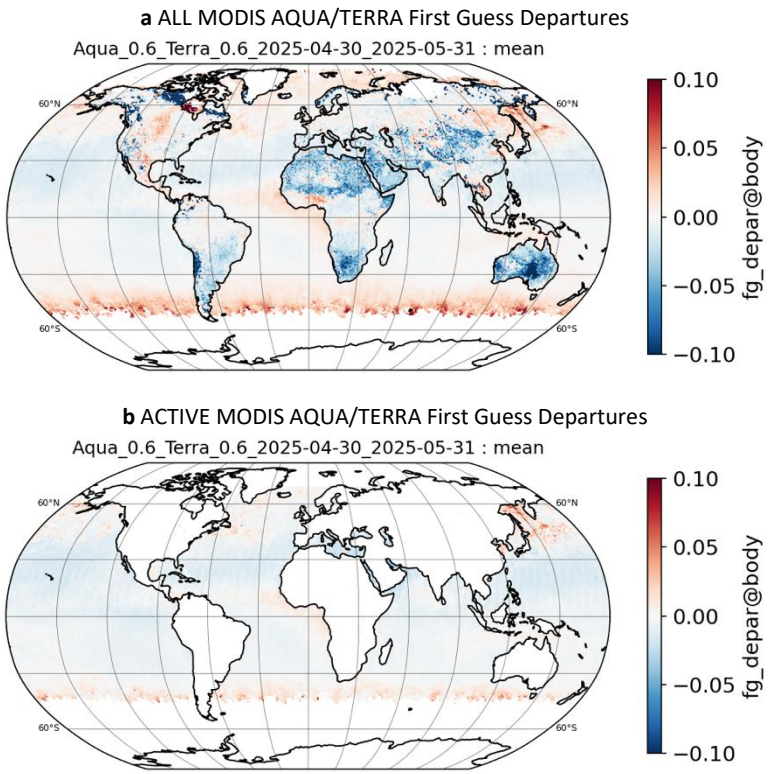

Figure **5** not only demonstrates the impact of observation screening but also reveals systematic bias patterns in the first guess departures. A small global negative bias is evident over the ocean in aerosol-clear scenes, which is further confirmed by the time series for both Aqua and Terra shown in Figure **6**. In contrast, the presence of aerosols introduces a larger positive bias, indicating that aerosol loading significantly influences reflectance departures.

Additional regional biases are observed around 50°S, likely associated with strong surface winds. These conditions can alter surface reflectance and aerosol distribution, contributing to localized discrepancies between observations and model equivalents.

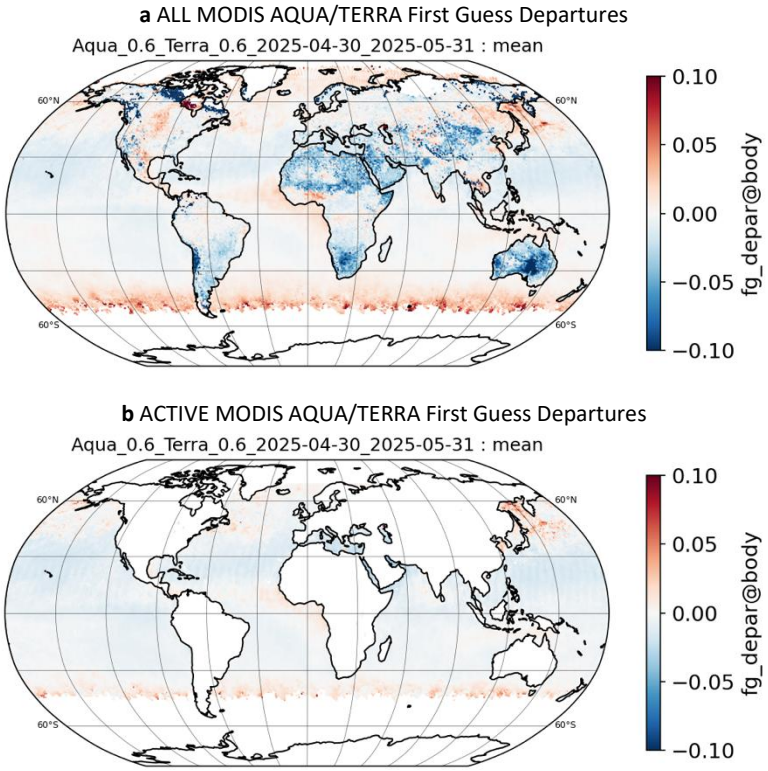

Figure 5. *MODIS on Aqua and Terra First Guess Departures averaged for May 2025 for all data (top) and active data (bottom) kept after applying data selection.*

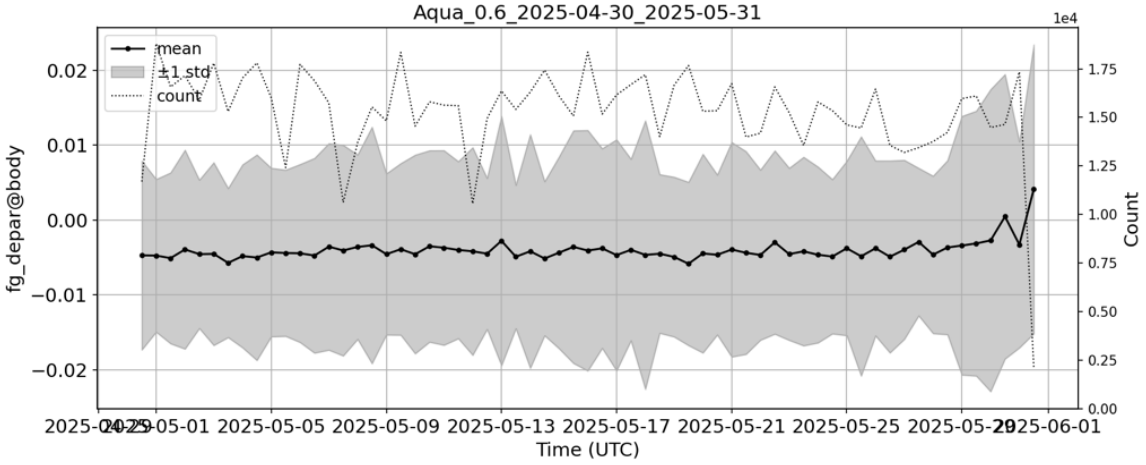

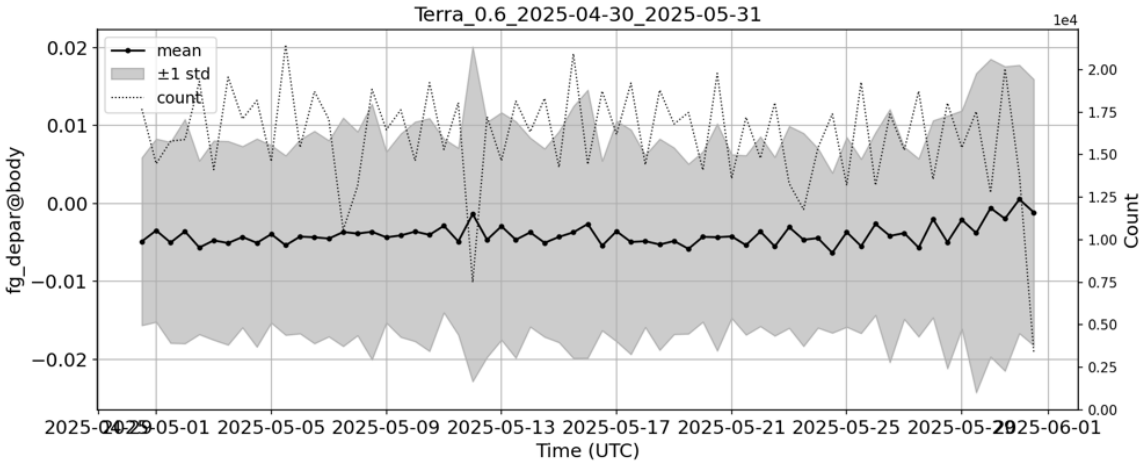

Figure 6. *Time series of First Guess Departures for MODIS on Aqua (top) and Terra (bottom) for May 2025.*

7.3 Assimilation results

Assimilation results over for the whole month of May and June are presented in this section. Figure 7 shows a six-panel comparison with the monthly mean first-guess departures, analysis departures, and departure reduction. Departure reduction is negative across the globe for both months, meaning the analysis is closer to the observation than the first-guess. A significant reduction can be seen in the Gulf of Guinea, north Atlantic and the west-coast of Africa.

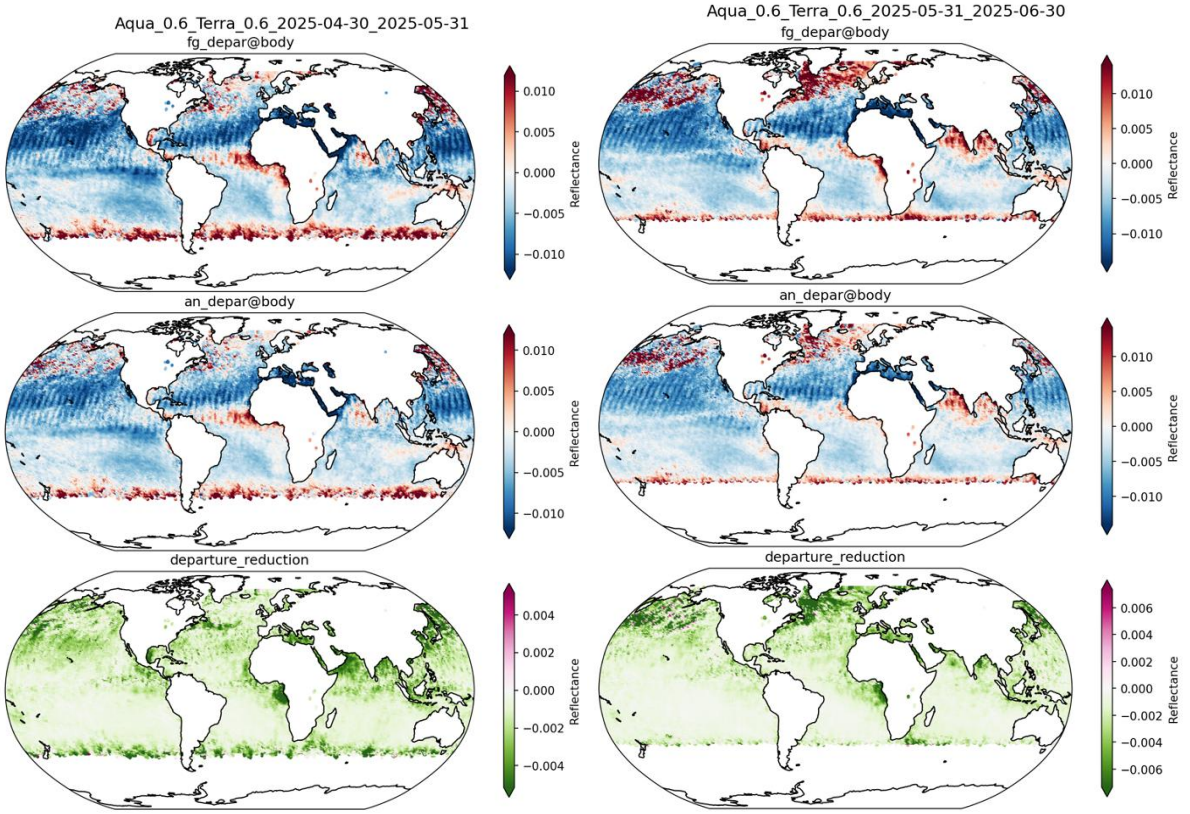

Figure 7. *Six-panel comparison illustrating the First Guess Departures (top row), Analysis Departures (middle row) and Departure Reduction (bottom row) for May 2025 (left column) and June 2025 (right column).*

7.4 Verification against ground-based observations

In this section, we present an evaluation performed with the CAMS Ver0D tool, which enables the verification of both aerosol forecasts and analyses against ground-based observations from the AERONET network (Holben et al., 1998; https://aeronet.gsfc.nasa.gov/). Although the network is spatially sparse in certain parts of the world and most stations are over land, it provides high-quality reference measurements of aerosol optical properties and is widely regarded as the state-of-the-art for aerosol validation.

Experiments included here were described in Table 1. It is worth reminding that the Baseline experiments include the assimilation of AOD from the various sensors as used in CAMS operations (eg, MODIS, PMAp, VIIRS), while the visible aerosol reflectance assimilation experiments -VIS_AER_RFL- only include level-2 reflectances from one single wavelength from MODIS. The control experiment does not include AOD nor visible aerosol reflectance assimilation.

Figure 8 depicts the temporal evolution of the global mean bias between forecasted and observed aerosol optical depth (AOD) at 550 nm, computed over the AERONET network for multiple experimental configurations. The assimilation of visible reflectances yields different results for the selected observation error values. VIS_AER_RFL_0.015 exhibits a smaller bias for most of May, while the VIS_AER_RFL_0.05 exhibits a smaller bias in June. When compared against the AOD assimilation results are mixed, but VIS_AER_RFL_0.015 shows smaller bias for most of the period evaluated. Control and VIS_AER_RFL_0.05 experiments show a larger negative bias during periods characterized by elevated aerosol loadings relative to the configuration assimilating AOD or the VIS_AER_RFL_0.015 experiment, such as late May and the first half of June.

Figure 9 is similar to Figure 8, but shows the global root mean square error (RMSE) values. Here the AOD assimilation experiment exhibits the smaller RMSE for most of the period. Visible reflectance assimilation shows, in general, lower RMSE than the control experiment, even beating the AOD experiment on specific days (eg, VIS_AER_RFL_0.015 on 6th June).

Figure 10 is similar to Figure 8, but focuses on Europe only rather than globally. Here, the VIS_AER_RFL_0.015 experiment shows the smallest bias for most of May (after the spin-up) and the first part of June. For the second half of June, biases are very similar for all experiments.

Figure 11 is similar to Figure 9, but focuses on Europe only rather than globally. In May, the VIS_AER_RFL experiments outperform the AOD one, while in June is the AOD one showing the smaller RMSE. However, the VIS_AER_RFL experiments perform comparably to the AOD experiment, even showing the smallest RMSE on the 7th June for the VIS_AER_RFL_0.015 experiment.

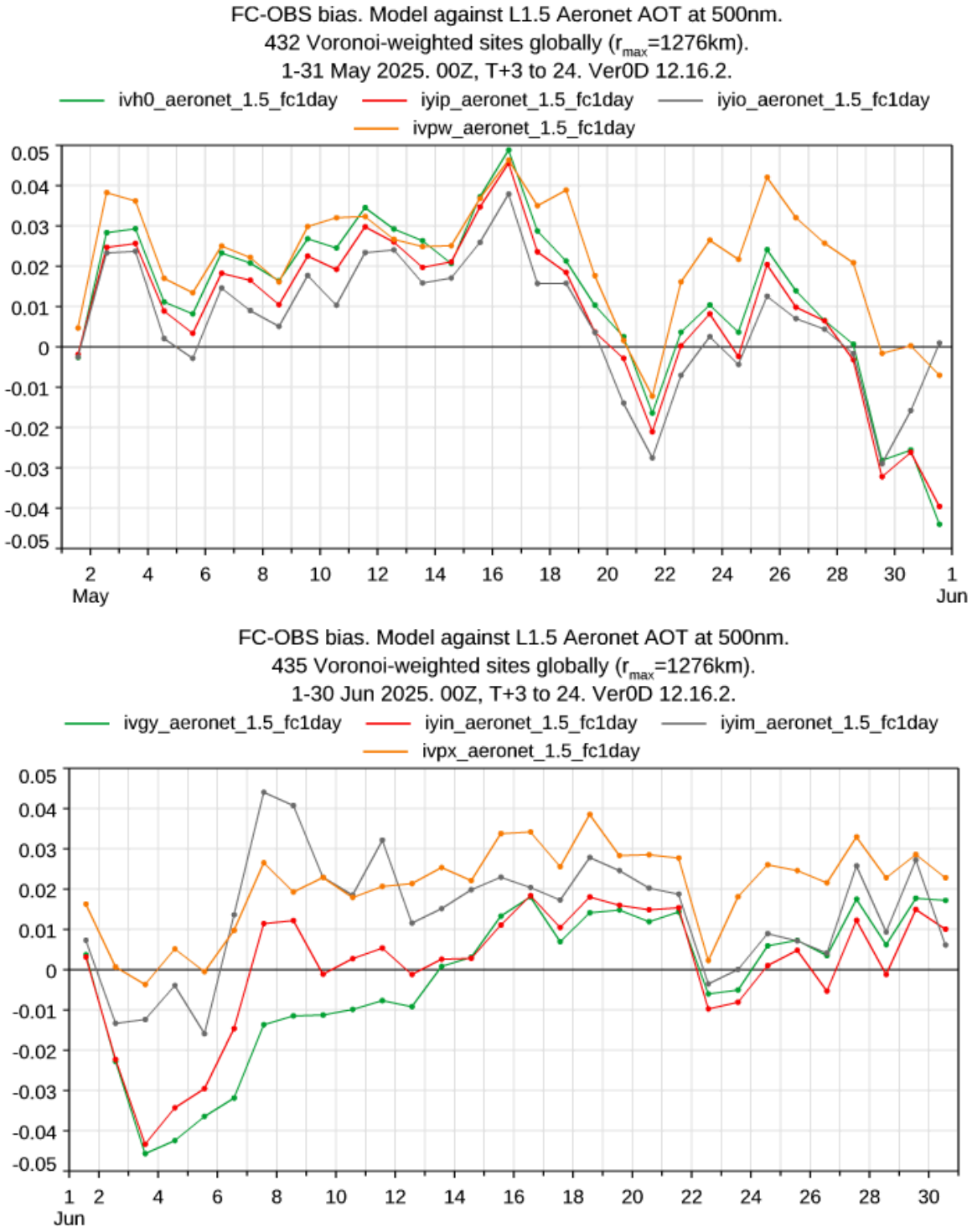

Figure 8. Time series of the global mean bias between forecasted and observed aerosol optical depth (AOD) at 550 nm, calculated over the AERONET network for different experimental configurations. The bias is defined as forecast minus observation and represents systematic deviations in model performance relative to ground-based measurements. Results are shown for May (upper panel) and June (lower panel). Each line corresponds to a distinct experiment: CONTROL (green), VIS_AER_RFL with obs_error=0.05 (red), VIS_AER_RFL with obs_error=0.015 (grey) and BASELINE (orange) (see ***Error! Reference source not found.*** *for further details), enabling intercomparison of forecast skill.*

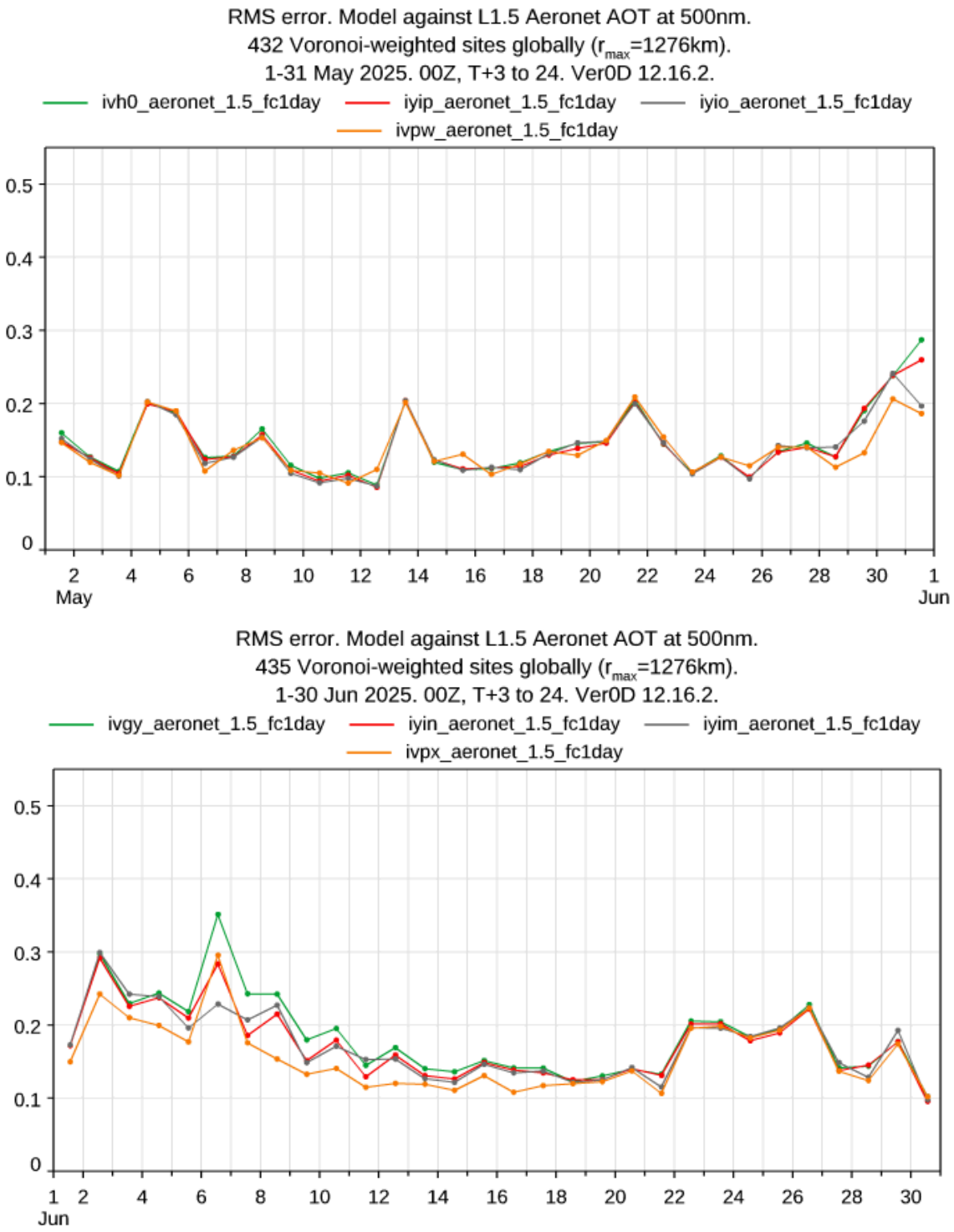

Figure 9. Time series of the global root mean square error between forecasted and observed aerosol optical depth (AOD) at 550 nm, calculated over the AERONET network for different experimental configurations. The bias is defined as forecast minus observation and represents systematic deviations in model performance relative to ground-based measurements. Results are shown for May (upper panel) and June (lower panel). Each line corresponds to a distinct experiment: Control (green), VIS_AER_RFL with obs_error=0.05 (red), VIS_AER_RFL with obs_error=0.015 (grey) and Baseline (orange) (see ***Error! Reference source not found.*** *for further details), enabling intercomparison of forecast skill.*

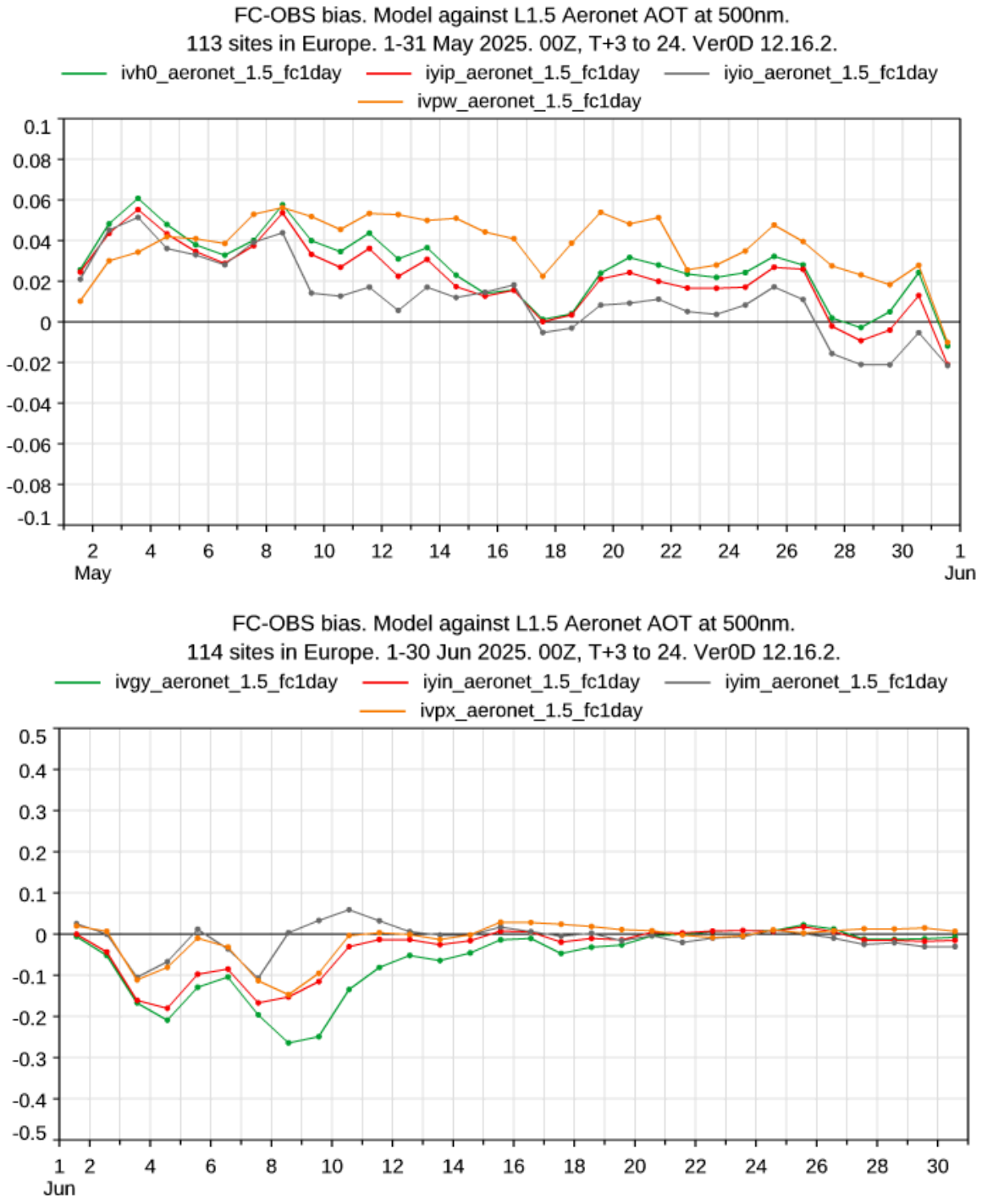

*Figure 10. Time series of the EUROPE mean bias between forecasted and observed aerosol optical depth (AOD) at 550 nm, calculated over the AERONET network for different experimental configurations. The bias is defined as forecast minus observation and represents systematic deviations in model performance relative to ground-based measurements. Results are shown for May (upper panel) and June (lower panel). Each line corresponds to a distinct experiment: Control (green), VIS_AER_RFL with obs_error=0.05 (red), VIS_AER_RFL with obs_error=0.015 (grey) and Baseline (orange) (see **Error! Reference source not found.** for further details), enabling intercomparison of forecast skill.*

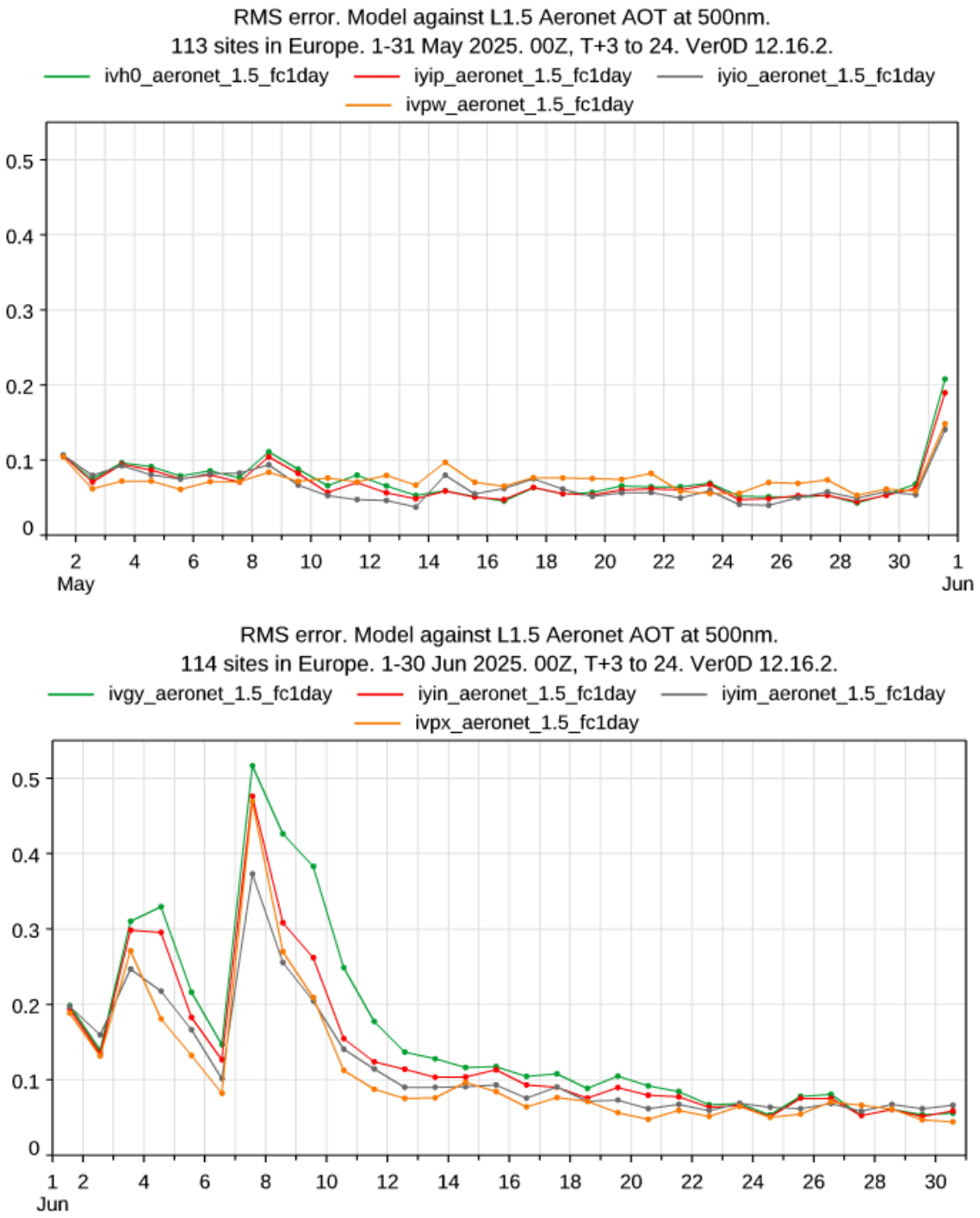

Figure 11. Time series of the EUROPE root mean square error between forecasted and observed aerosol optical depth (AOD) at 550 nm, calculated over the AERONET network for different experimental configurations. The bias is defined as forecast minus observation and represents systematic deviations in model performance relative to ground-based measurements. Results are shown for May (upper panel) and June (lower panel). Each line corresponds to a distinct experiment: Control (green), VIS_AER_RFL with obs_error=0.05 (red), VIS_AER_RFL with obs_error=0.015 (grey) and Baseline (orange) (see ***Error! Reference source not found.*** *for further details), enabling intercomparison of forecast skill.*

7.5 Case study: dust event on 4th June 2025

A robust way to assess aerosol assimilation performance is through targeted case studies of significant events. One such example is the Saharan dust outbreak on 4th June 2025.

Figure 12 illustrates this case using a four-panel layout for the VIS_AER_RFL_0.015 experiment:

- First Guess Simulated Reflectance: the model simulation shows the highest reflectance intensity in the same region identified by observations, indicating that the aerosol signal is captured in the background state.
- MODIS Observations: the satellite measurements confirm the presence of a strong dust plume over the affected area.
- Analysis increments: showing the increase (positive) -or decrease (negative)- of the aerosol concentration in the analysis due the assimilation.
- Independent FCI Composite: Provides independent qualitative/ visual validation for the presence of a large aerosol load, confirming the spatial extent of the dust outbreak.

Figure 13 shows the departure reduction, ie., the analysis departures minus background departures for the two different observation error values. VIS_AER_RFL_0.015 demonstrates a greater positive impact of assimilation, with significant reductions in observation-model differences after incorporating visible reflectances when compared to VIS_AER_RFL_0.05.

This case highlights the ability of the assimilation system to improve aerosol representation and reduce biases when visible reflectances are assimilated.

Figure 14 presents the time series of AOD at 550 nm at the Mindelo_OSCM AERONET station in Cape Verde for the different experimental configurations. This site is strategically positioned to capture Saharan dust outbreaks. None of the experiments successfully reproduces the full intensity of the dust events, indicating limitations in the representation of extreme dust episodes within the tested assimilation approaches.

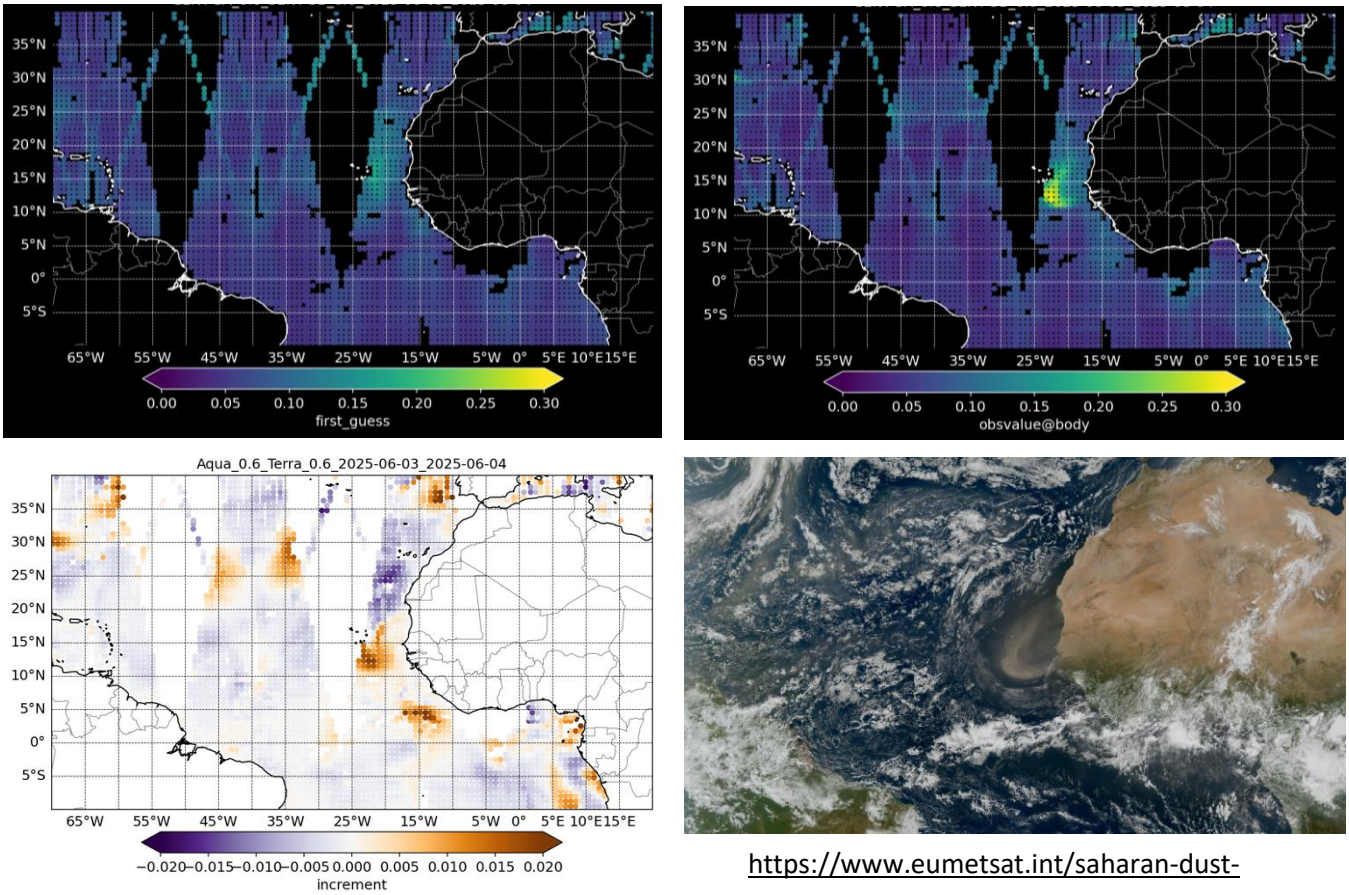

https://www.eumetsat.int/saharan-dust-

Figure 12. *Four-panel comparison illustrating the assimilation of MODIS visible reflectances (665 nm). Top-left: First Guess Simulated Reflectance; Top-right: MODIS Observations; Bottom-left: Analysis increments; Bottom-right: Independent FCI composite observation highlighting a dust outbreak.*

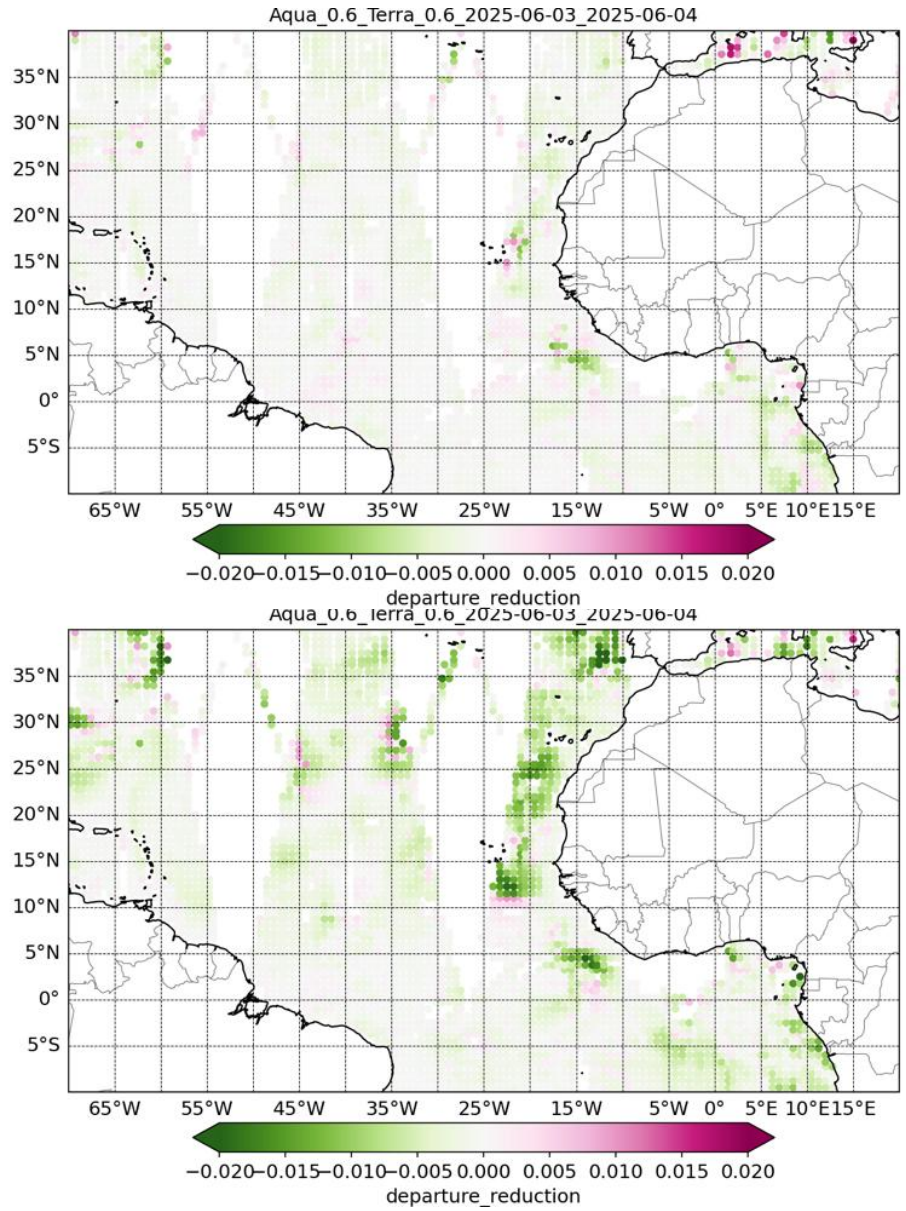

Figure 13. *Departure Reduction* ($|\boldsymbol{d_A}| - |\boldsymbol{d_B}|$) *in the experiments assimilating aerosol visible reflectances for different observation error values: 0.05 (top) and 0.015) (bottom) during the dust outbreak on 4th June 2025.*

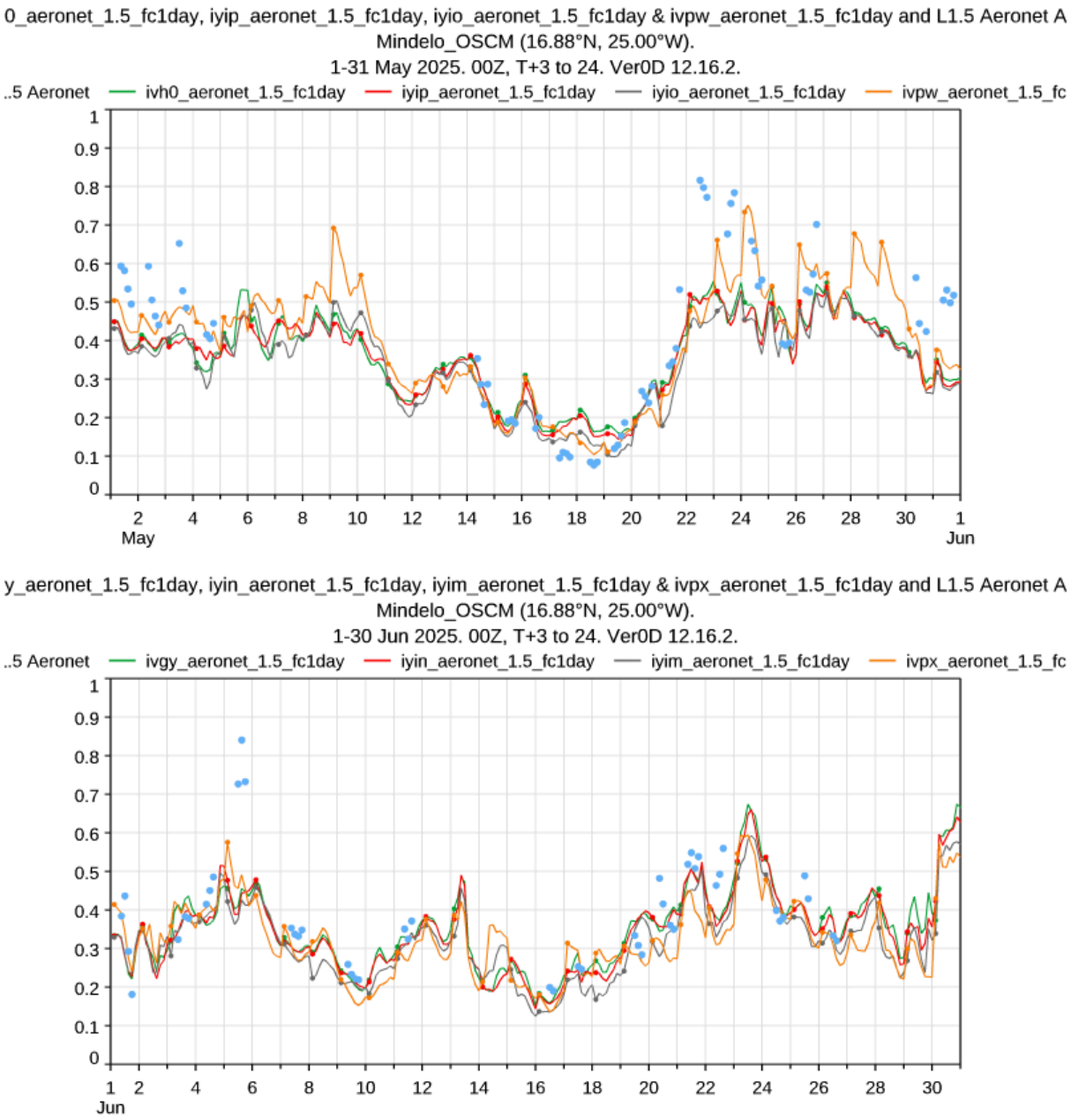

Figure 14. Time series of aerosol optical depth (AOD) at 550 nm at the Mindelo_OSCM AERONET station. Each solid corresponds to the forecasted model values for each experiment: Control (green), VIS_AER_RFL with obs_error=0.05 (red), VIS_AER_RFL with obs_error=0.015 (grey) and Baseline (orange) (see ***Error! Reference source not found.*** *for further details), while AERONET observations are represented by blue markers. Results are shown for May (upper panel) and June (lower panel). This comparison highlights the temporal variability of AOD and the ability of each configuration to reproduce observed aerosol conditions.*

8 Conclusions and next steps

In this document, we have set out a description of all the elements required for the implementation of a prototype assimilation system for AVRAS:

- The implementation and testing of the MFASIS-Aerosol fast radiative transfer code for aerosol reflectances
- The selection of the observation option to be used
- The preparation of the visible reflectance observations to fit in the visible BUFR template created for this purpose
- The configuration and running of the assimilation experiments
- The evaluation of the assimilation results.

This work represents the first implementation of aerosol visible observation processing in the IFS using RTTOV-MFASIS. Previous studies relied on Oxford-RAL retrievals and served primarily as demonstrators. However, there are still some caveats. MODIS-specific radiative transfer MFASIS-Aerosol coefficients are not yet available; therefore, coefficients from Meteosat-11 were used as a proxy in these experiments. Only 9 CAMS aerosol species were used in the training for the development of this version of MFASIS-Aerosols, which lags behind compared to the current 16 species CAMS configuration.

The results presented should be regarded as preliminary and based on a suboptimal configuration, which includes incomplete observation screening, missing variational quality control and variational bias correction, and a lack of fine-tuning of observation errors. Consequently, these findings should be interpreted as a proof of concept rather than definitive scientific conclusions. Despite this caveat, huge progress has been made in CAMEO in bringing the Technology Readiness Level (TRL) for direct aerosol reflectance assimilation from level 1 to level 5.

We can identify two key milestones. First, the implementation of substantial technical developments enabling visible reflectance monitoring and assimilation within the Integrated Forecasting System (IFS). This includes the integration of MFASIS-Aerosols, adaptation of RTTOV-14 interfaces, and creation of bespoke data flows for MODIS visible observations. Second, this is the first successful demonstration of aerosol visible monitoring and assimilation using the RTTOV-MFASIS framework, showcasing improved aerosol representation and reduced observation-model discrepancies in case studies such as the Saharan dust outbreak.

We can summarize the next steps and future goals in the following three:

i) Scientific evaluation and expansion: Perform a comprehensive scientific evaluation using the correct MFASIS-Aerosol coefficient files for relevant periods, focusing on high-impact events such as dust outbreaks. Expand the aerosol species representation from 9 to 16 species to better align with the current CAMS configuration, improving consistency between aerosol modelling and assimilation. Explore the integration of additional sensors, such as VIIRS or OLCI on Sentinel 3A and 3B (provided that a level 2 cloud-cleared reflectance product is made available), to broaden observational coverage and enhance data diversity.

ii) Multi-channel extension: Extend monitoring and assimilation capabilities beyond the 0.6 μm channel, incorporating additional visible wavelengths to exploit the full information content of satellite reflectances. Assess the sensitivity of different channels to aerosol properties and their potential impact on assimilation performance.

iii) Refinement of assimilation system: Build upon promising initial trials by refining the assimilation framework: improved quality control (QC), implementing advanced screening techniques to ensure robust observation selection, bias correction to

address systematic biases identified in the first guess departures, and error specification to improve observation and background error characterization to optimize assimilation impact.

9 References

Benedetti, A., S. Quesada-Ruiz, J. Letertre-Danczak, M. Matricardi & G. Thomas, 2020: Progress towards assimilating visible radiances, ECMWF Newsletter No. 162, 10. https://www.ecmwf.int/en/newsletter/162/news/progresstowards-assimilating-visible-radiances

Desroziers, G., L. Berre, B. Chapnik, & P. Poli, 2005: Diagnosis of observation, background and analysis-error statistics in observation space. Q.J.R. Meteorol. Soc., 131: 3385-3396. https://doi.org/10.1256/qj.05.108

Holben, B.N., T.F. Eck, I. Slutsker, D. Tanré, J.P. Buis, A. Setzer, E. Vermote, J.A. Reagan, Y.J. Kaufman, T. Nakajima, F. Lavenu, I. Jankowiak & A. Smirnov, 1998: AERONET - A Federated Instrument Network and Data Archive for Aerosol Characterization, Remote Sensing of Environment, Volume 66, Issue 1, 1998, Pages 1-16, ISSN 0034-4257, https://doi.org/10.1016/S0034-4257(98)00031-5

Scheck, L., 2021: A neural network based forward operator for visible satellite images and its adjoint, J. Quant. Spectrosc. Ra., 274, 107841. https://doi.org/10.1016/j.jqsrt.2021.107841

Turner, E., 2025: Diverse profile datasets from the ECMWF CAMS 137-level short range forecasts. Technical Report NWPSAF-EC-TR-044. https://nwp-saf.eumetsat.int/downloads/profiles/nwpsaf_cams137_2025_doc.pdf

Document History

Version	Author(s)	Date	Changes
0.1	Samuel Quesada-Ruiz, Angela Benedetti, Cristina Lupu, Tobias Necker	14 Nov 2025	Initial version
0.2	Samuel Quesada-Ruiz, Angela Benedetti, Cristina Lupu, Tobias Necker	28 Nov 2025	Revised and updated version including comments from the internal reviewers
1.0	Samuel Quesada-Ruiz, Angela Benedetti, Cristina Lupu, Tobias Necker	30 Nov 2025	V1.0 issued

Internal Review History

Internal Reviewers	Date	Comments
Zhuyun Ye, Camilla Geels (AU)	24 Nov 2025	
Oriol Jorba (BSC)		
Jeronimo Escribano (BSC)	21 Nov 2025	Very nice work delivering preliminary scientific outcomes and demonstrating potential for further improvement, even though it was a highly technical task.